J. Wind Eng. Ind. Aerodyn. ▮ (▮▮▮▮) ▮▮▮–▮▮▮

Contents lists available at ScienceDirect

Journal of Wind Engineering and Industrial Aerodynamics

journal homepage: www.elsevier.com/locate/jweia

Numerical study on flow fields of tornado-like vortices using the LES turbulence model

Takeshi Ishihara [a], Sho Oh [a,*], Yoshiteru Tokuyama [b]

[a] Department of Civil Engineering, School of Engineering, The University of Tokyo, 7-3-1, Hongo, Bunkyo-ku, Tokyo, Japan
[b] M&T Co., LTD, Art Center of Tokyo Building, 11F, 1-4-1, Senju, Adachi-ku, Tokyo, Japan

ARTICLE INFO

Keywords:
Numerical tornado simulator
LES turbulence model
Flow field
Force balance

ABSTRACT

Flow fields of tornado-like vortices generated by a numerical tornado simulator have been investigated using the LES turbulence model for two typical swirl ratios. The core radii of simulated vortices with swirl ratios of 0.31 and 0.65 showed favorable agreement with visualized vortices by a laboratory tornado simulator. Mean velocity fields were examined to obtain detailed corner flow patterns. It was found that an one-cell type vortex with a central upward flow appears for the case of low swirl ratio and vertical velocities show peaks at the center of the vortex, while a two-cell type vortex with a central downward flow emerges for the case of high swirl ratio and the maximum tangential velocity appears near ground. The formations of one-cell and two-cell type vortices were investigated by examining the axisymmetric time averaged Navier–Stokes equations. The vertical pressure gradient generates vertical velocities at the center of vortex in the one-cell type vortex, whereas the centrifugal force balances with the radial pressure gradient and the vertical advection term of the radial velocity in case of the two-cell type vortex.

1. Introduction

Tornados are vortices with strong three-dimensional flow fields and cause severe damages compared to other wind induced disasters. Wind resistant design of structures requires proper consideration of tornado-induced wind loads and tornado-borne missiles, which need detailed information of the three-dimensional flow field of a tornado. Many researchers have performed the laboratory and numerical simulations in order to obtain the detailed information of the flow field.

In laboratory simulation, Ward (1972) first developed a laboratory simulator with a fan at the top to generate updraft and guide-vanes near the floor to provide angular momentum, and succeeded in generation of many types of tornado-like vortex observed in nature. Wan and Chang (1972) replaced the guide-vanes with rotating screen, and measured radial, tangential and vertical velocities with a three-dimensional velocity probe. They found that vertical velocities near the vortex axis remain all positive and become strong for low swirl ratio, and are negative for high swirl ratio. Mitsuta and Monji (1984) modified the simulator so that rotation is given at the top of the simulator, and showed occurrence of the maximum tangential velocity near the ground surface for two-cell type vortex. Recently Matsui and Tamura (2009) have conducted velocity measurement for tornado-like vortex generated by Ward-type simulator with Laser Doppler Velocimeter (LDV). Haan et al. (2008) have developed a large laboratory simulator with guide-vanes at the top to generate vortex. In their study, the measurements of flow structure in the vortex were validated by comparing with mobile Doppler radar observations of two major tornados. However, in laboratory simulation, it was difficult to obtain detailed three-dimensional velocity and pressure field due to the strong turbulence motion near the surface and the center of the vortex.

Recently numerical simulations have been conducted extensively to study the tornado-vortex dynamics. Howells et al. (1988) and Nolan and Farrell (1999) used axisymmetric Navier–Stokes equation with constant viscosity in cylindrical coordinate to investigate the flow field of tornado-like vortex. Low-swirl intense vortex (one-cell type vortex) and drowned vortex jump (two-cell type vortex) were reproduced by Nolan and Farrell (1999). Lewellen and Lewellen (1997, 2007) used LES turbulence model to examine the sensitivity of vortex structure to swirl ratio and translation speed. Lewellen et al. (1999) also used the LES model to study the influence of local swirl ratio and interaction of the surface roughness. Kuai et al. (2008) used the $k-\varepsilon$ model to study parameter sensitivity for the flow field of a laboratory-simulated tornado. They showed that the numerical approach can

* Corresponding author.
E-mail addresses: ishihara@bridge.t.u-tokyo.ac.jp (T. Ishihara), s.oh@bridge.t.u-tokyo.ac.jp (S. Oh), yoshiteru.tokuyama@jpmandt.com (Y. Tokuyama).

0167-6105/$ - see front matter © 2011 Elsevier Ltd. All rights reserved.
doi:10.1016/j.jweia.2011.01.014

be used to simulate the surface winds of a tornado and to control certain parameters of the laboratory simulator to influence the tornado characteristics. However, the comparison between the numerical and laboratory-simulated tornados is insufficient and mechanism of the formation of flow field has not been fully revealed.

This paper presents a numerical Ward-type tornado simulator and the detailed information of three-dimensional flow fields in two typical tornado-like vortices obtained using LES turbulence model. Section 2 describes the numerical model used in this study. In Section 3, the three-dimensional flow fields are examined and compared with the experimental data to verify the performance of numerical model. Finally axisymmetric time averaged Navier–Stokes equations are evaluated to reveal the mechanism of the formation of flow field in Section 4.

2. Numerical model

2.1. Governing equations

The governing equations employed in LES model are obtained by filtering the time-dependent Navier–Stokes equations as follows:

$$\frac{\partial \rho \tilde{u}_i}{\partial x_i} = 0 \tag{1}$$

$$\frac{\partial}{\partial t}(\rho \tilde{u}_i) + \frac{\partial}{\partial x_j}(\rho \tilde{u}_i \tilde{u}_j) = \frac{\partial}{\partial x_j}\left(\mu \frac{\partial \tilde{u}_i}{\partial x_j}\right) - \frac{\partial \tilde{p}}{\partial x_i} - \frac{\partial \tau_{ij}}{\partial x_j} \tag{2}$$

where $\tilde{u}_i$ and $\tilde{p}$ are filtered mean velocity and filtered pressure respectively. ρ is density, τ_{ij} is subgrid-scale stress and is modeled as follows:

$$\tau_{ij} = -2\mu_t \tilde{S}_{ij} + \frac{1}{3}\tau_{kk}\delta_{ij}, \quad \tilde{S}_{ij} \equiv \frac{1}{2}\left(\frac{\partial \tilde{u}_i}{\partial x_j} + \frac{\partial \tilde{u}_j}{\partial x_i}\right) \tag{3}$$

where μ_t is subgrid-scale turbulent viscosity, and $\tilde{S}_{ij}$ is the rate-of-strain tensor for the resolved scale.

Smagorinsky–Lilly model is used for the subgrid-scale turbulent viscosity

$$\mu_t = \rho L_s^2 |\tilde{S}| = \rho L_s \sqrt{2\tilde{S}_{ij}\tilde{S}_{ij}}, \quad L_s = \min\left(\kappa\delta, C_s V^{1/3}\right) \tag{4}$$

where L_s is the mixing length for subgrid-scales, κ is the von Karman constant, 0.42, C_s is Smagorinsky constant, δ is the distance to the closest wall and V is the volume of a computational cell. In this study, C_s is determined as 0.032 based on Oka and Ishihara (2009).

2.2. Boundary conditions near wall and solution procedure

Finite volume method and unstructured collocated mesh are used for the present simulations. semi-implicit pressure linked equations (SIMPLE) algorithm is employed for solving the discritized equations (Ferziger and Peric, 2002). The pressure at inlet of the convergence region is zero, and velocity at the outlet of the simulator is given as 9.55 m/s to generate upward flow in the tornado. Three velocity components and the pressure are set as zero for the initial conditions. In this study, grid-refinement was conducted and the temporal independence in the solution was systematically analyzed by change in the time interval. As a result, velocity profiles were almost unchanged.

When a wall-adjacent cell is in the laminar sublayer, the wall shear stress is obtained from the laminar stress–strain relationship as follows:

$$\frac{\overline{u}}{u_\tau} = \frac{\rho u_\tau y}{\mu} = y^+$$

If the mesh cannot resolve the laminar sublayer, it is assumed that the centroid of the wall-adjacent cells fall within the logarithmic region of the boundary layer, and the law-of-the-wall is employed.

$$\frac{\overline{u}}{u_\tau} = \frac{1}{k}\ln E\left(\frac{\rho u_\tau y}{\mu}\right)$$

where $\overline{u}$ is the filtered velocity tangential to wall, u_τ is the friction velocity, κ (von Karman constant) is 0.42, and the constant E is 9.793.

In the tornado-like vortex, a flow with both axial and radial pressure gradients appears, but the radial pressure gradient is dominant comparing with the axial pressure gradient in the near surface region, which implies the wall function can be used. In most of the region, the wall-adjacent cells are in the laminar sublayer. The maximum of y^+ is 26 in the core region of the vortex.

2.3. Configurations of the numerical tornado simulator

In this study, Ward-type tornado simulator is numerically modeled including the guide-vanes and the honeycomb. Fig. 1 shows the overview of the numerical tornado simulator used in this study. The configuration and dimensions are exactly same as the laboratory simulator used by Matsui and Tamura (2009). Fig. 2(a) and (b) shows three-dimensional view and top view of bottom surface of mesh used in the simulation. In order to quantitatively evaluate the turbulent flow in the vortex, the minimum size of mesh are set about 2 and 1 mm in radial and vertical directions, respectively. Higher mesh density is used at center and the floor to capture the vortex structure. Parameters used in this simulation are shown in Table 1.

Swirl ratio is an important parameter to determine the structure of a tornado-like vortex. The swirl ratio defined

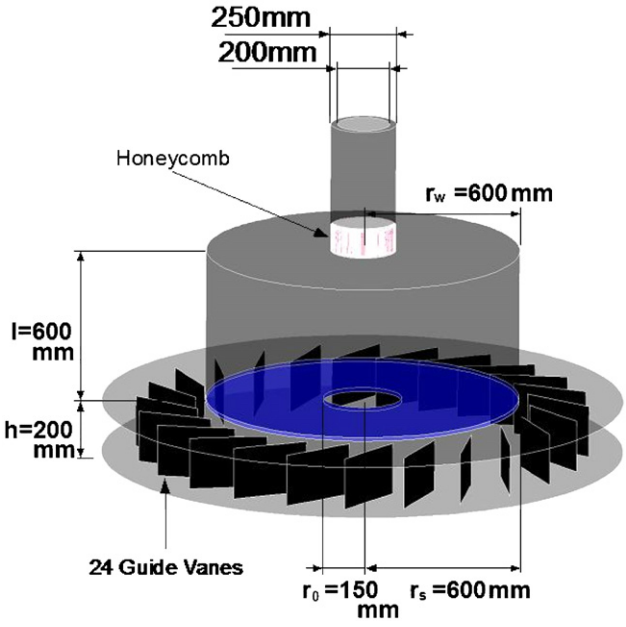

Fig. 1. Overview of the numerical tornado simulator.

Please cite this article as: Ishihara, T., et al., Numerical study on flow fields of tornado-like vortices using the LES turbulence model. J. Wind Eng. Ind. Aerodyn. (2011), doi:10.1016/j.jweia.2011.01.014

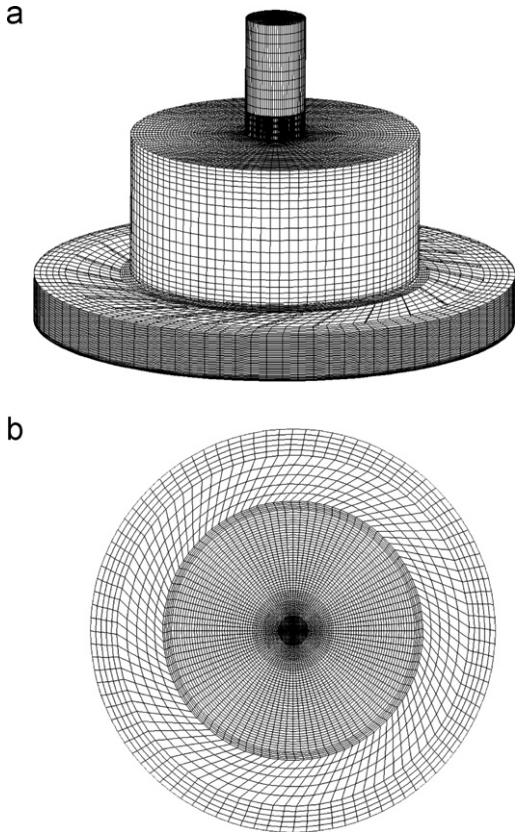

Fig. 2. Mesh used in the numerical simulation. (a) Three-dimensional view and (b) top view of bottom surface.

Table 1
Parameters used in this simulation.

Reynolds number	$\mathrm{Re}=W_0D/\nu=1.63\times10^5$
Non-dimensional time step	$\Delta tW_0/D=0.016$
Convergence criteria	5×10^{-4}
Mesh size in the radial direction	2.08–26 mm
Mesh size in the vertical direction	0.98–5.0 mm

by Ward (1972) is used in this study as follows:

$$S=\frac{\tan\theta}{2a} \tag{5}$$

where θ is the angle of the guide-vane, and a is the aspect ratio of the inflow height, h, to the radius of the hole, r_0. Two representative swirl ratios are chosen to examine the different type of the structure of vortex. The case of $S=0.31$ represents a low swirl ratio vortex and the case of $S=0.65$ denotes a high swirl ratio one.

Comparisons of the instantaneous streamlines calculated from the numerical results and the flow visualizations by Matsui and Tamura (2009) are shown in Fig. 3. Streamlines and flow visualizations show that the core radius is small for the low swirl ratio case and large for the high swirl ratio one. The shape of the vortices shows satisfactory resemblance, indicating that the numerical simulator can generate tornado-like vortex similar to the laboratory simulator. Table 2 shows representative values used in this study, where V_c is the maximum tangential velocity at the radius of r_c in a cyclostrophic balance region.

3. Mean velocity field and pressure field

In order to examine flow field in the tornado-like vortices, the normalized mean velocities as well as pressures are discussed and compared with the laboratory data in this section. Experimental results obtained by Mitsuta and Monji (1984) and Matsui and Tamura (2009) are used for the validation of numerical model. Mitsuta and Monji (1984) measured the vertical velocity using hot-wire anemometer, while Matsui and Tamura (2009) measured the tangential velocity using the Laser Doppler Velocimeter.

The flow patterns strongly depend on the swirl ratio. The predicted velocity vectors in radial–vertical plane are shown in Fig. 4 for the two swirl ratios. For the case of $S=0.31$, the boundary layer inflow penetrates all the way to the center axis ($r=0$), then turns upward into a strong draft, forming an one-cell type vortex as shown in Fig. 4(a). On the other hand, for the case of $S=0.65$ the boundary layer inflow also penetrates to the central axis ($r=0$) and turns upward, but the vertical flow breaks

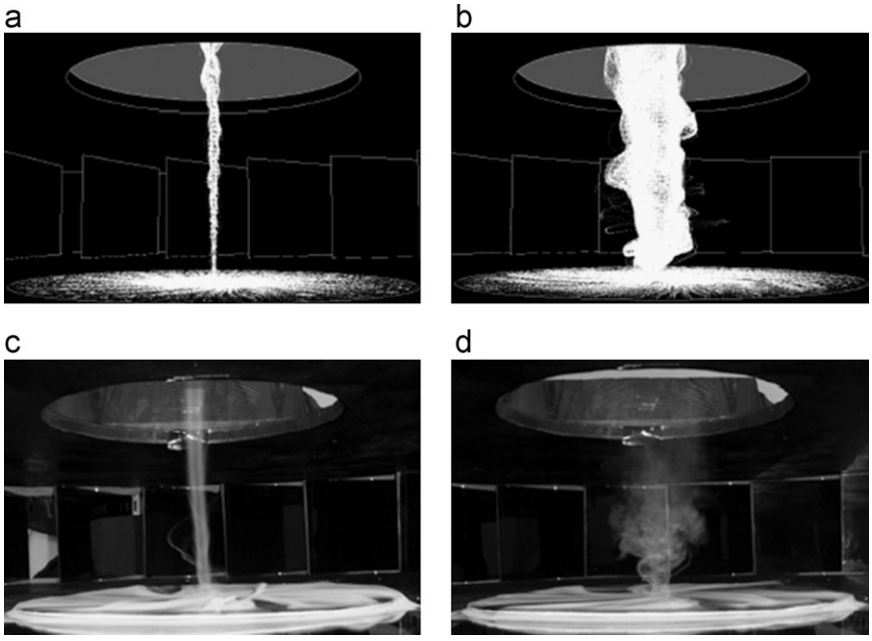

Fig. 3. Comparison of streamlines for (a) $S=0.31$ and (b) $S=0.65$ calculated by the numerical simulation and flow visualizations for (c) $S=0.31$ and (d) $S=0.65$.

Please cite this article as: Ishihara, T., et al., Numerical study on flow fields of tornado-like vortices using the LES turbulence model. J. Wind Eng. Ind. Aerodyn. (2011), doi:10.1016/j.jweia.2011.01.014

away from the vertical axis at $z=0.2r_c$ and a downward flow occurs in the center of the vortex generating a two-cell type vortex as shown in Fig. 4(b). In order to examine the flow field in vortices, radial, and vertical distributions as well as the contour of normalized velocity components and pressure are shown in Figs. 5–8 for both swirl ratios.

3.1. Tangential velocity

Normalized tangential velocities in radial and vertical direction as well as the contours in radial–vertical plane are shown in Fig. 5. Velocity distributions at higher elevations are almost same as shown in Fig. 5(a) and (b), and predicted tangential velocities agree satisfactorily with the laboratory data by Matsui and Tamura (2009). In the surface layer, tangential velocities decrease in the case of $S=0.31$, whereas they increase in the case of $S=0.65$. The maximum value for $S=0.65$ reaches to $1.4V_c$ at $z=0.2r_c$. This increase in the tangential velocity near the surface is important for wind resistant design, since most of the engineering structures exist in this region. The profiles of vertical distribution of tangential velocity in the case of $S=0.31$ are similar to regular turbulent flow over a long flat plane as shown in Fig. 5(c). On the other hand, the velocities inside the vortex in case of $S=0.65$ increase near the ground surface as shown in Fig. 5(d).

3.2. Radial velocity

Fig. 6 shows normalized radial velocities in radial and vertical direction as well as the contours in radial–vertical plane. In the case of $S=0.31$, the radial velocities are all negative and decreases with the increase in height as shown in Fig. 6(a) and (c). The maximum value appears at an elevation of $z=0.2r_c$ and reaches to $0.5V_c$. On the other hand, in the case of $S=0.65$, a strong inflow can be observed near the ground surface, and the radial velocities become positive near the center of the vortex at lower height. The absolute values of maximum negative radial velocities are close to V_c as shown in Fig. 6(d). The maximum normalized radial velocities in the case of $S=0.31$ are found in agreement with those proposed by Simiu and Scanlan (1996), whereas large radial velocities are observed in the case of $S=0.65$.

Table 2
Representative values used in this study.

Case	r_0 (mm)	h (mm)	a	θ (°)	S	V_c (m/s)	r_c (mm)
1	150	200	1.33	40	0.31	13.0	8.33
2	150	200	1.33	60	0.65	8.3	32.6

3.3. Vertical velocity

Normalized vertical velocities in radial and vertical direction as well as the contours in radial–vertical plane are shown in Fig. 7. In the case of $S=0.31$, the vertical velocities take their maximum values at the center of the vortex and increase with the increase of height as shown in Fig. 7(a) and (c). The maximum vertical velocity is about $1.9V_c$ at $z=2r_c$. On the other hand, the vertical velocities for $S=0.65$, as shown in Fig. 7(b) and (d), show their maximum values close to $0.6V_c$, which are almost same as the value of $0.67V_c$ proposed by Simiu and Scanlan (1996). The normalized vertical velocities from the laboratory by Mitsuta and Monji (1984) are also plotted in Fig. 7(b) for comparison and the predicted velocities show satisfactory agreement with the measured ones at $z=1.3r_c$.

3.4. Pressure

Fig. 8 shows the normalized pressures in radial and vertical directions as well as the contours in radial–vertical plane. In the case of $S=0.31$, pressures decrease rapidly with the increase in height as shown in Fig. 8(a), while pressures at various heights are almost same in the case of $S=0.65$ as shown in Fig. 8(b). Fig. 8(c)–(f) describes distinct differences between these two cases, that result in different flow fields.

4. Force balances in the tornado-like vortices

Considering the tornado induced damages to the structures, the high wind speeds observed in the numerical tornado simulator are important and their mechanisms have to be revealed. In this section, axisymmetric time-averaged Navier–Stokes equations are derived and the force balance is investigated to explain the mechanism of those phenomena.

4.1. Vertical force balance

To examine the mechanism of the high vertical velocity at the center of the vortex in the case of $S=0.31$, vertical components of the axisymmetric Navier–Stokes equation is derived as

$$U\frac{\partial W}{\partial r}+W\frac{\partial W}{\partial z}=-\frac{1}{\rho}\frac{\partial P}{\partial z}-\left(\frac{\partial uw}{\partial r}+\frac{\partial w^2}{\partial z}+\frac{uw}{r}\right)+D_w \tag{6}$$

where u, v, and w denote the radial, tangential, and vertical component of fluctuating velocity, z is the height above ground, and r is the radius from the central axis.

The left hand side consists of radial (A_{rw}) and vertical (A_{zw}) advection terms. The right hand side of the equation is the

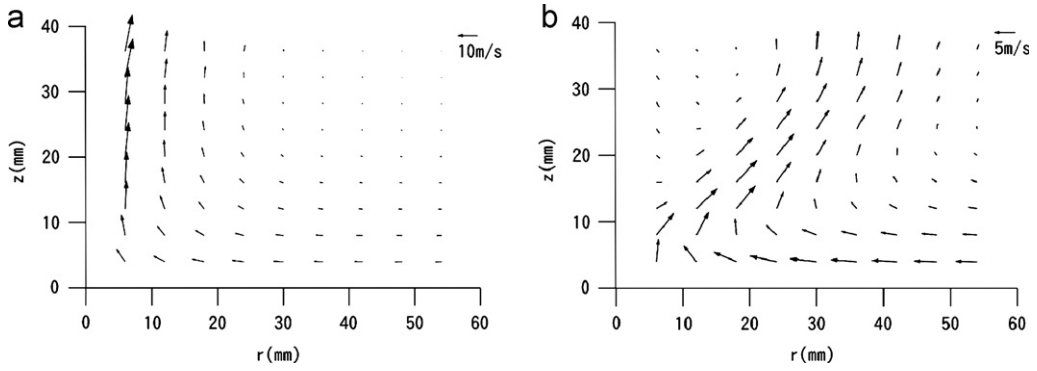

Fig. 4. Axisymmetric time-averaged velocity vector in radial–vertical plane: (a) $S=0.31$ and (b) $S=0.65$.

Please cite this article as: Ishihara, T., et al., Numerical study on flow fields of tornado-like vortices using the LES turbulence model. J. Wind Eng. Ind. Aerodyn. (2011), doi:10.1016/j.jweia.2011.01.014

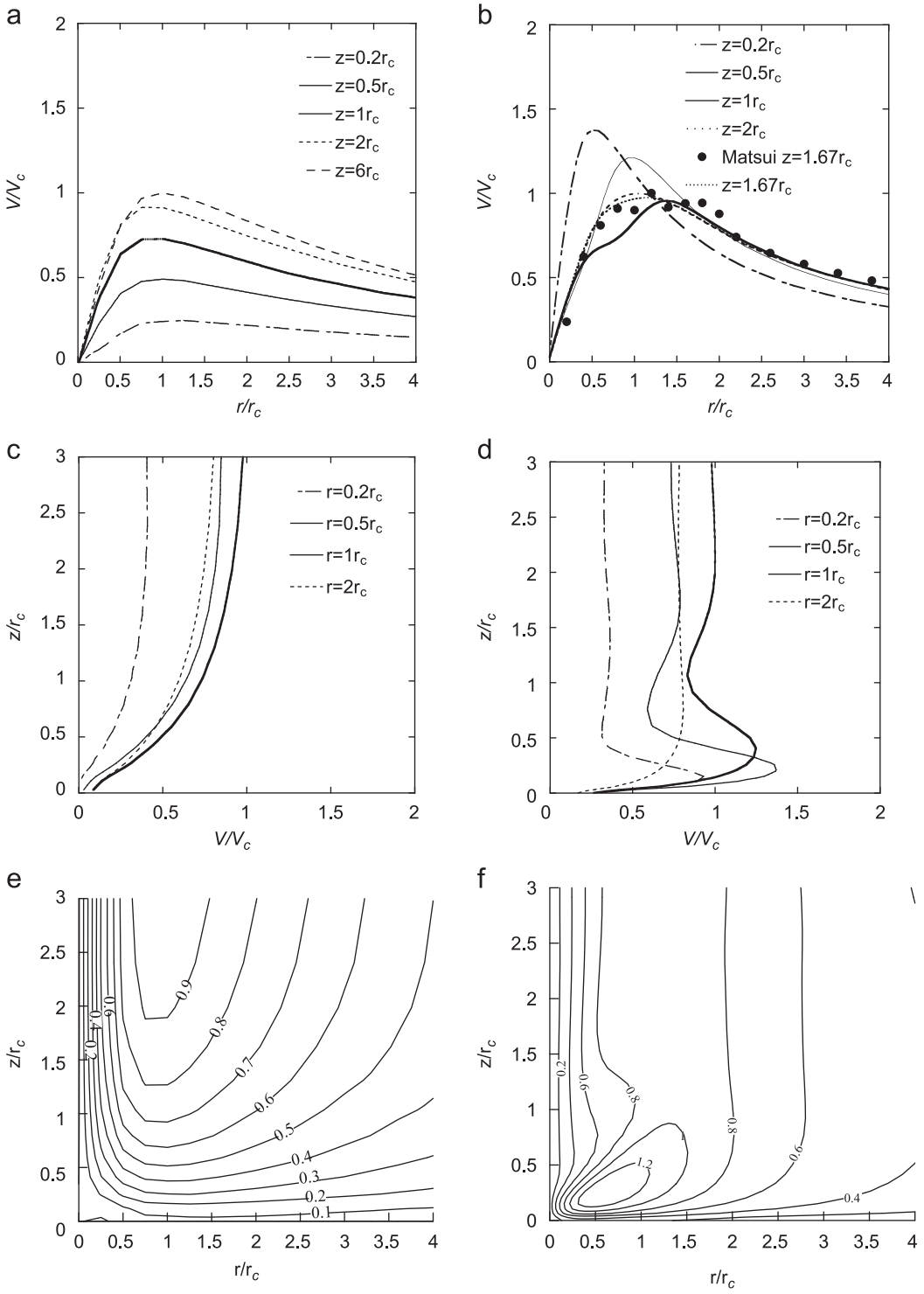

Fig. 5. Normalized tangential velocity: (a) and (b) radial distribution, (c) and (d) vertical distribution, (e) and (f) contour in radial–vertical plane for $S=0.31$ and $S=0.65$, respectively.

vertical pressure gradient term (P_z), Reynolds stress term (T_w), and the diffusion term (D_w). For the low swirl ratio case, each term on the vortex axis is estimated and shown in Fig. 9(a). Among all the terms, the contribution from the vertical pressure gradient and the vertical advection terms is dominant. This indicates that this equation can be approximated as the balance equation of vertical pressure gradient and the vertical advection. From this balance, the vertical wind velocity, W, can be predicted as

$$W=\sqrt{2\int\left(-\frac{1}{\rho}\frac{\partial P}{\partial z}\right)dz}=\sqrt{2\frac{P_s-P}{\rho}} \tag{7}$$

where P_s is the pressure at surface and P is pressure at the height of z obtained from simulation. The vertical velocity calculated from the pressure gradient using this model and the simulated

Please cite this article as: Ishihara, T., et al., Numerical study on flow fields of tornado-like vortices using the LES turbulence model. J. Wind Eng. Ind. Aerodyn. (2011), doi:10.1016/j.jweia.2011.01.014

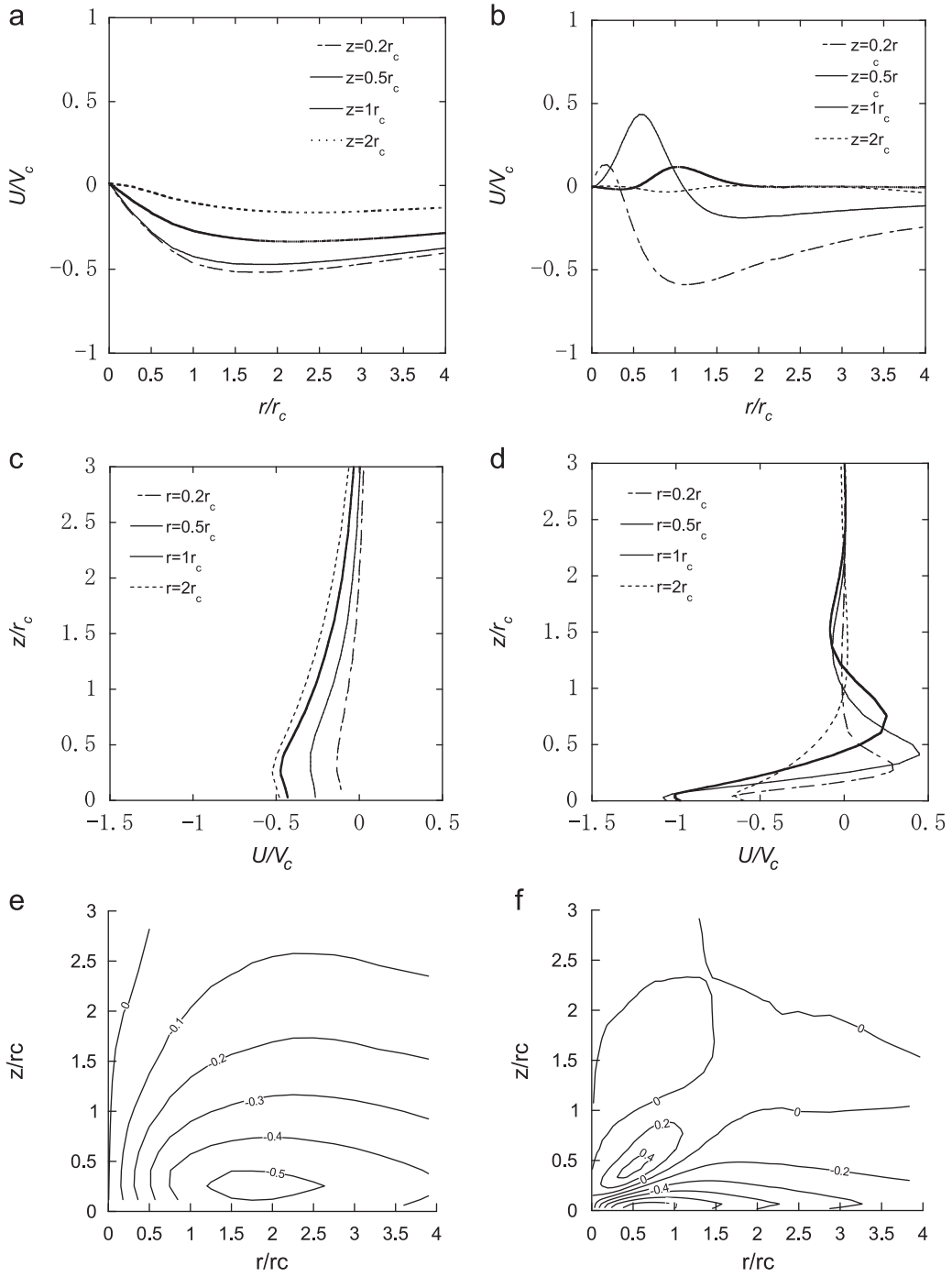

Fig. 6. Normalized radial velocity: (a) and (b) radial distribution, (c) and (d) vertical distribution, (e) and (f) contour in radial–vertical plane for $S=0.31$ and $S=0.65$, respectively.

vertical velocity are shown in Fig. 9(b). The proposed model shows good agreement with the simulation, which suggests the large vertical velocity in case of $S=0.31$ is formed by the large pressure gradients.

4.2. Radial force balance

The mechanism of the strong tangential velocity in the high swirl ratio case is investigated by considering the force balance of radial component of Navier–Stokes equation. The radial term of the axisymmetric Navier–Stokes equation can be written as

$$U\frac{\partial U}{\partial r}+W\frac{\partial U}{\partial z}-\frac{V^2}{r}=-\frac{1}{\rho}\frac{\partial P}{\partial r}-\left(\frac{\partial u^2}{\partial r}+\frac{\partial uw}{\partial z}-\frac{v^2}{r}+\frac{u^2}{r}\right)+D_u \quad (8)$$

The left hand side of this equation consists of the radial (A_{ru}) and vertical (A_{zu}) advection term and the centrifugal force term (C_r). The right hand side of the equation is the radial pressure gradient term (P_r), Reynolds stress term (T_u), and the diffusion term (D_u). Each term at $z=3r_c$ in the cyclostrophic balance region is estimated and shown in Fig. 10(a) for the high swirl ratio case. The centrifugal force and the pressure gradient are almost

Please cite this article as: Ishihara, T., et al., Numerical study on flow fields of tornado-like vortices using the LES turbulence model. J. Wind Eng. Ind. Aerodyn. (2011), doi:10.1016/j.jweia.2011.01.014

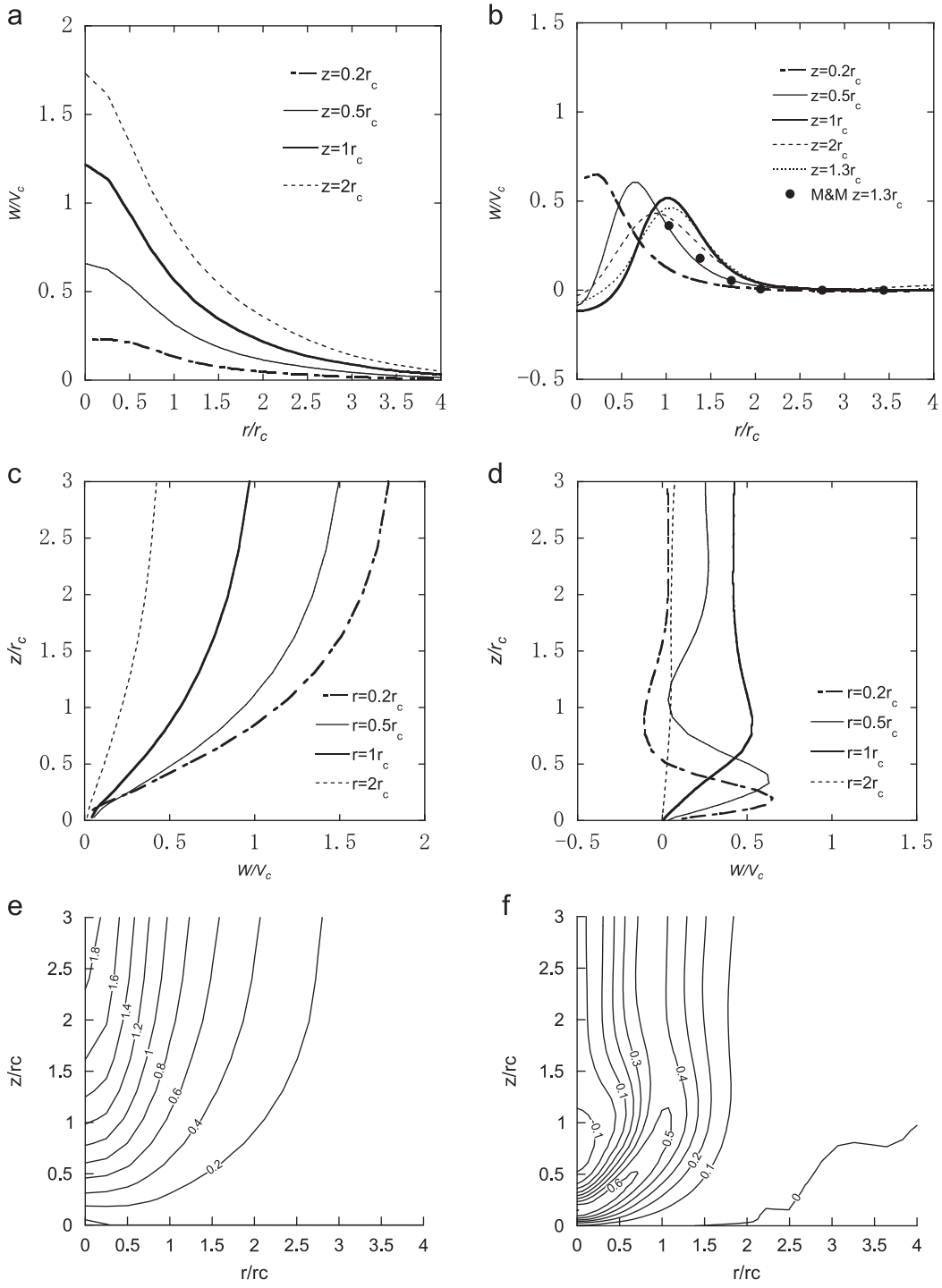

Fig. 7. Normalized vertical velocity: (a) and (b) radial distribution, (c) and (d) vertical distribution, (e) and (f) contour in radial–vertical plane for $S=0.31$ and $S=0.65$, respectively.

balanced at this elevation, and the tangential velocity, V, obtained from this balance shows good agreement with the numerical simulation as shown in Fig. 10(b). Near the ground surface, the centrifugal force is the largest term and balances with the pressure gradient term and the vertical advection term as shown in Fig. 11(a). From this balance, the tangential velocity near ground, V, can be estimated as

$$V=\sqrt{V_p^2+V_A^2}=\sqrt{\frac{1}{\rho}\frac{\partial P}{\partial r}r+W\frac{\partial U}{\partial z}r} \tag{9}$$

The calculated tangential velocity based on the model shows good agreement with the simulated one as shown in Fig. 11(b). The tangential velocity, V_p, is smaller than the simulated one when the tangential velocity is estimated by the pressure gradient term. This indicates that the increase of tangential velocity near the surface in the two-cell type vortex comes from the vertical advection term (A_{zu}). The mechanism of the flow field can be explained such that pressure gradient is independent of the height and the ground pressure gradient does not balance with the centrifugal force because of the friction. As a result, large

Please cite this article as: Ishihara, T., et al., Numerical study on flow fields of tornado-like vortices using the LES turbulence model. J. Wind Eng. Ind. Aerodyn. (2011), doi:10.1016/j.jweia.2011.01.014

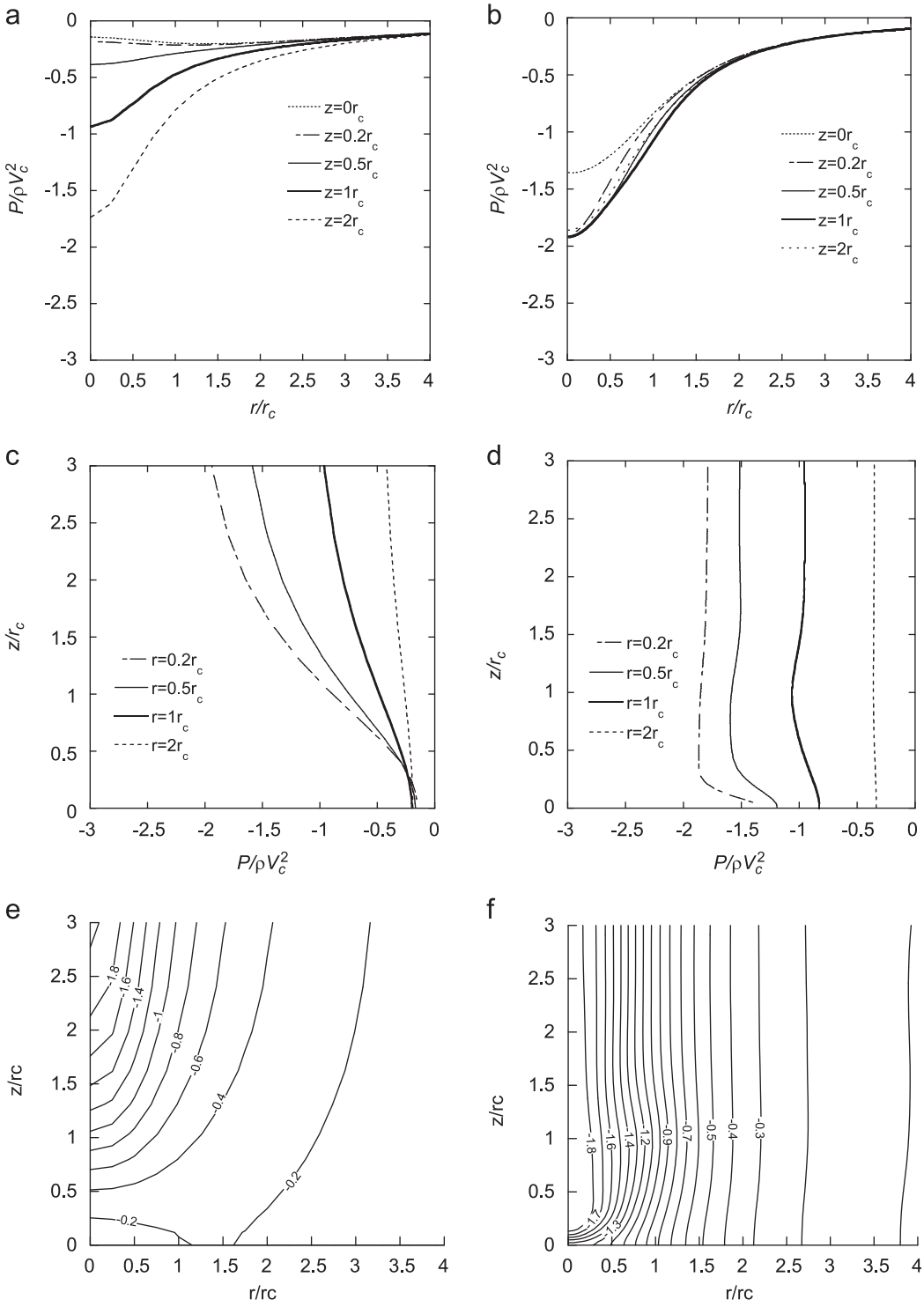

Fig. 8. Normalized pressure: (a) and (b) radial distribution, (c) and (d) vertical distribution, (e) and (f) contour in radial–vertical plane for $S=0.31$ and $S=0.65$, respectively.

radial inflow occurs near the ground and causes an increase in the tangential velocity there.

5. Conclusion

In this study, flow fields of tornado-like vortices generated by a numerical tornado simulator have been investigated using the LES turbulence model for two typical swirl ratios. Following conclusions were obtained.

The core radii of vortices with swirl ratios of 0.31 and 0.65 from the numerical tornado simulator agree favorably with visualized vortices of the laboratory simulator.

An one-cell type vortex appears for the low swirl ratio case, in which the vertical velocities show peaks at the center and the tangential velocity decreases as the height decreases. On the other hand, a two-cell type vortex appears for the high swirl ratio case, in which the maximum tangential velocity appears at the level close to the ground and the peaks of vertical velocity are observed near the radius of maximum tangential wind.

Please cite this article as: Ishihara, T., et al., Numerical study on flow fields of tornado-like vortices using the LES turbulence model. J. Wind Eng. Ind. Aerodyn. (2011), doi:10.1016/j.jweia.2011.01.014

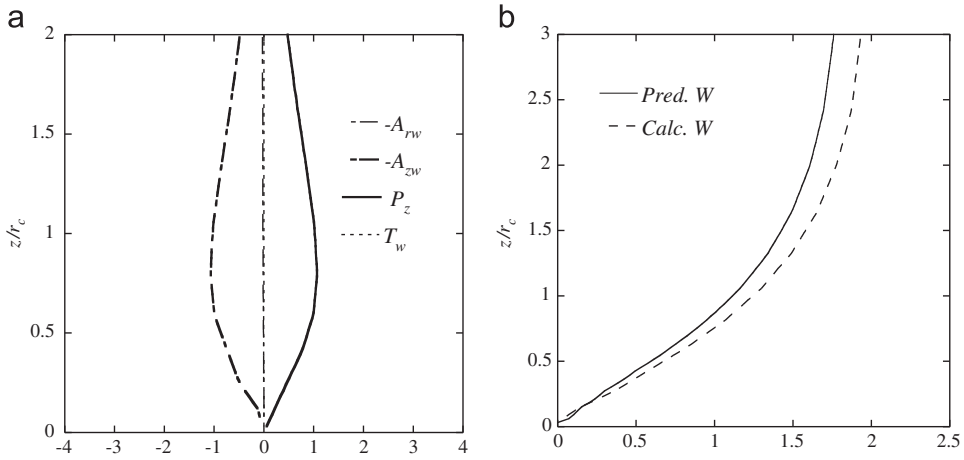

Fig. 9. Vertical distribution of (a) normalized vertical forcing terms of Navier–Stokes equation and (b) comparison of simulated and calculated vertical velocities at the center of the vortex ($r=0$) for $S=0.31$.

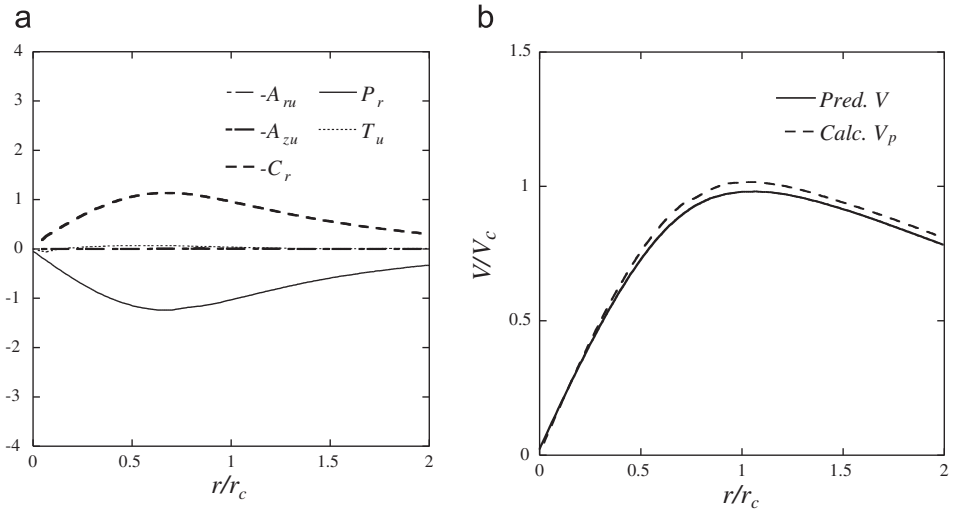

Fig. 10. Radial distribution of (a) normalized radial forcing terms of Navier–Stokes equation and (b) comparison of simulated and calculated tangential velocities at $z=3r_c$ in the cyclostrophic balance region for $S=0.65$.

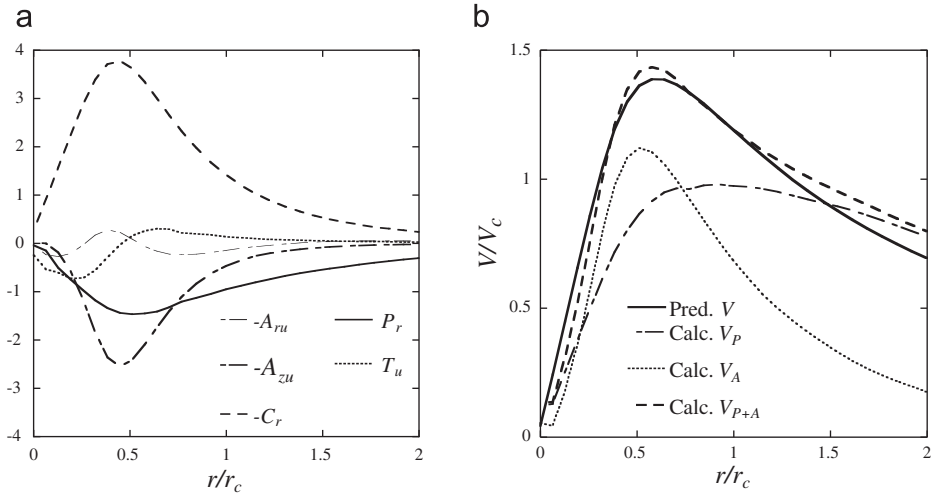

Fig. 11. Radial distribution of (a) normalized radial forcing terms of Navier–Stokes equation and (b) comparison of simulated and calculated tangential velocities at $z=0.25r_c$ near the ground surface for $S=0.65$.

Please cite this article as: Ishihara, T., et al., Numerical study on flow fields of tornado-like vortices using the LES turbulence model. J. Wind Eng. Ind. Aerodyn. (2011), doi:10.1016/j.jweia.2011.01.014

The maximum vertical velocity is generated by the vertical pressure gradient and reaches 1.9 times of V_c for the low swirl ratio case. On the other hand, the centrifugal force balances with the radial pressure gradient and the vertical advection term of the radial velocity, and the maximum value for the tangential velocities close to the ground becomes as high as 1.4 times of V_c for the high swirl ratio case.

References

Ferziger, J., Peric, M., 2002. Computational Method for Fluid Dynamics third ed. Springer.

Haan, F.L., Sarkar, P.P., Gallus, W.A., 2008. Design, construction and performance of a large tornado simulator for wind engineering applications. Engineering Structures 30, 1146–1159.

Howells, P.C., Rotunno, R., Smith, R.R., 1988. A comparative study of atmospheric and laboratory analogue numerical tornado-vortex models. Quarterly Journal of Royal Meteorological Society 114, 801–822.

Kuai, L., Haan, F.L., Gallus, W.A., Sarkar, P.P., 2008. CFD simulations of the flow field of a laboratory simulated tornado for parameter sensitivity studies and comparison with field measurements. Wind and Structures 11 (2), 1–22.

Lewellen, D.C., Lewellen, W.S., 1997. Large-eddy simulation of a tornado's interaction with the surface. Journal of the Atmospheric Sciences 54 (5), 581–605.

Lewellen, D.C., Lewellen, W.S., Xia, J., 1999. The influence of a local swirl ratio on tornado intensification near the surface. Journal of the Atmospheric Sciences 57, 527–544.

Lewellen, D.C., Lewellen, W.S., 2007. Near-surface intensification of tornado vortices. Journal of the Atmospheric Sciences 64, 2176–2194.

Matsui, M., Tamura, Y., 2009. Influence of swirl ratio and incident flow conditions on generation of tornado-like vortex. In: Proceedings of EACWE 5, CD-ROM.

Mitsuta, Y., Monji, N., 1984. Development of a laboratory simulator for small scale atmospheric vortices. Natural Disaster Science 6, 43–54.

Nolan, D.S., Farrell, B.F., 1999. The structure and dynamics of tornado-like vortices. Journal of the Atmospheric Sciences 56, 2908–2936.

Oka, S., Ishihara, T., 2009. Numerical study of aerodynamic characteristics of a square prism in a uniform flow. Journal of Wind Engineering and Industrial Aerodynamics 97, 548–559.

Simiu, E., Scanlan, R.N., 1996. Wind Effects on Structures: Fundamental and Applications to Design third ed. John Wiley and Sons, 497pp.

Wan, C.A., Chang, C.C., 1972. Measurement of the velocity field in a simulated tornado-like vortex using a three-dimentional velocity probe. Journal of Atmospheric Science 29, l16–127.

Ward, N.B., 1972. The exploration of certain features of tornado dynamics using a laboratory model. Journal of the Atmospheric Sciences 29, 1194–1204.

Please cite this article as: Ishihara, T., et al., Numerical study on flow fields of tornado-like vortices using the LES turbulence model. J. Wind Eng. Ind. Aerodyn. (2011), doi:10.1016/j.jweia.2011.01.014